

Electric-field-induced long-lived spin excitations in two-dimensional spin-orbit coupled systems

P. Kleinert

Paul-Drude-Institut für Festkörperelektronik, Hausvogteiplatz 5-7, 10117 Berlin, Germany

V. V. Bryksin*

A. F. Ioffe Physical Technical Institute, Politekhnicheskaya 26, 194021 St. Petersburg, Russia

(Received 1 August 2008; revised manuscript received 18 November 2008; published 28 January 2009)

Rigorous coupled spin-charge drift-diffusion equations are derived from quantum-kinetic equations for the spin-density matrix that incorporate effects due to k -linear spin-orbit interaction, an electric field, and the elastic scattering on nonmagnetic impurities. The explicit analytical solution for the induced magnetization exhibits a pole structure, from which the dispersion relations of spin excitations are identified. Applications of the general approach refer to the excitation of long-lived field-induced spin waves by optically generated spin and charge patterns for a planar and cylindrical geometry. This approach transfers methods known in the physics of space-charge waves to the treatment of long-lived spin eigenmodes that appear in planar and nonplanar two-dimensional electron systems with spin-orbit interaction. In addition, the amplification of an oscillating electric field by spin injection is demonstrated.

DOI: [10.1103/PhysRevB.79.045317](https://doi.org/10.1103/PhysRevB.79.045317)

PACS number(s): 72.25.Dc, 72.20.My, 72.10.Bg

I. INTRODUCTION

Recent attention has focused on semiconductor spintronics, in which electronic spin polarization is used for information processing. Especially, the generation and manipulation of nonequilibrium spin densities by exclusively electrical means in nonmagnetic semiconductors is particularly attractive. Progress toward the development of spintronic devices depends on theoretical and experimental studies of effects due to the spin-orbit interaction (SOI). This spin-dependent coupling gives rise to an internal effective magnetic field that leads to spin precession and reorientation. For semiconductor quantum wells or heterostructures, the bulk and structural inversion asymmetry result in Dresselhaus and Rashba SOI terms, respectively. Unfortunately, the very same SOI also causes spin relaxation. The randomization of electron spins is due to the fact that the SOI depends on the in-plane momentum k . Consequently, the precession frequencies differ for spins with different wave vectors. This so-called inhomogeneous broadening in conjunction with any elastic and inelastic scattering causes spin dephasing.¹ The details of which depend on the character of dominating scattering processes, the band structure, and the crystal orientation.² In GaAs/Al_xGa_{1-x}As quantum wells grown along the [001] axis and with balanced Rashba and Dresselhaus SOI strengths, a strong anisotropy in the in-plane spin dephasing time has been measured.³⁻⁵ The spin relaxation along the [110] direction is efficiently suppressed. Based on this effect, which is robust due to an exact spin rotation symmetry of the spin-orbit Hamiltonian,⁶ a nonballistic spin-field-effect transistor was proposed.⁷ From a theoretical point of view, it is predicted that for an idealized model with k -linear SOI the spin polarization along [110] is conserved for a certain wave vector.⁶ The experimental confirmation of this prediction⁸ was possible by exploiting transient spin-grating techniques. This experimental method offers an efficient tool for identifying coupled spin-charge eigenstates in the two-dimensional electron gas (2DEG). Optically induced diffraction patterns are formed in semiconductors when two pulses with identical

energies interfere on the sample and excite electron-hole pairs.⁹⁻¹² By varying the relative angle between the two pump beams, the grating period can be tuned for resonant excitation of the eigenmodes. With a third time-delayed pulse that diffracts from the photoinjected spin or charge pattern, the time evolution of the spin polarization can be monitored. A free-carrier concentration grating is produced within the sample by two beams with parallel linear polarization. Alternatively, an oscillating spin polarization, which levitates over a homogeneous carrier ensemble, is generated by cross linearly polarized pump pulses. By detuning the frequencies, a moving (oscillating) charge and/or spin pattern can be produced.

Most interesting both for basic research and the application point of view are weakly damped spin-charge coupled eigenmodes of the semiconductor heterostructure. These excitations drastically change their character when an electric field acts simultaneously on spin and charge carriers. Similar to the traditional study of space-charge waves in crystals (see, for instance, Ref. 13), the field-dependent spin modes can be identified and excited by an experimental setup that provides the appropriate wave vector. Such an approach can profit from methods developed in the well-studied field of space-charge waves in crystals.

The reservoir of interesting spin phenomena is not exhausted by the treatment of a planar 2DEG with SOI. A diversity of new spin effects arises for different geometries of the 2DEG. In dependence on the curvature of the surface, in which the 2DEG resides, additional contributions to the SOI appear that may lead to new characteristic features. Examples of current interest provide microtubes fabricated by exploiting the self-rolling mechanism of strained bilayers. These rolled-up structures exhibit pronounced optical resonances¹⁴ arising from micron-sized cylindrical resonators or give rise to novel magnetoresistance oscillations, which were observed in the ballistic transport of electrons on cylindrical surfaces.¹⁵ For nonballistic spintronic device applications, the prediction of a conserved spin component, which arises when the Rashba coupling constant α equals the

quantity $\hbar^2/2m^*R$ (with R being the radius of the cylinder and m^* the effective mass of the 2DEG) is the most interesting.¹⁶ The identification of this novel long-lived spin mode by fabricated curved samples seems to be feasible with the present-day technology.^{17–20}

It is the aim of this paper to systematically derive general spin-charge coupled drift-diffusion equations for a semiconductor heterostructures with a general \mathbf{k} -linear SOI that refer both to the planar and cylindrical geometries. Based on the rigorous analytical solution of these equations, a number of electric-field-driven long-lived spin resonances are studied.

II. DERIVATION AND SOLUTION OF DRIFT-DIFFUSION EQUATIONS

In this section, we introduce the model, derive quantum-kinetic equations for the spin-density matrix, and solve related spin-charge coupled drift-diffusion equations for conduction-band electrons, which reside in an asymmetric semiconductor quantum well or in a heterostructure on a cylindrical surface. Coupled spin and charge excitations are treated by an effective-mass Hamiltonian, which includes both SOI and short-range spin-independent elastic scattering on impurities. We focus on spin effects exerted by an electric field \mathbf{E} . The single-particle model Hamiltonian for both the planar and cylindrical 2DEG has the form

$$H_0 = \sum_{k,s} a_{k_s}^\dagger [\varepsilon_k - \varepsilon_F] a_{k_s} + \sum_{k,s,s'} [\mathbf{\Omega}(\mathbf{k}) \cdot \boldsymbol{\sigma}_{ss'}] a_{k_s}^\dagger a_{k_s'} - ie\mathbf{E} \sum_{k,s} \nabla_{\boldsymbol{\kappa}} a_{k-(\boldsymbol{\kappa}/2)s}^\dagger a_{k+(\boldsymbol{\kappa}/2)s} |_{\boldsymbol{\kappa}=0} + u \sum_{k,k'} \sum_s a_{k_s}^\dagger a_{k's}, \quad (1)$$

where the carrier creation ($a_{k_s}^\dagger$) and annihilation (a_{k_s}) operators depend on the spin index s and the wave vector $\mathbf{k} = (k_x, k_y, 0)$ [$\mathbf{k} = (k_\varphi, k_z, 0)$] of the planar [cylindrical] 2DEG. k_z denotes the wave vector component along the cylinder axis and $k_\varphi = (m+1/2)/R$, with m being an integer. In Eq. (1), ε_k , ε_F , and $\boldsymbol{\sigma}$ denote the energy of free electrons, the Fermi energy, and the vector of Pauli matrices, respectively. In the Born approximation, the elastic-scattering time τ is expressed by the strength u of elastic scattering according to the equation

$$\frac{1}{\tau} = \frac{2\pi u^2}{\hbar} \sum_{k'} \delta(\varepsilon(\mathbf{k}) - \varepsilon(\mathbf{k}')). \quad (2)$$

All information about SOI is absorbed into the definition of the vector $\mathbf{\Omega}(\mathbf{k})$. The components of which have their specific form for the planar and cylindrical geometry. We restrict the treatment to linear-in- \mathbf{k} Rashba and Dresselhaus SOI contributions that result from the inversion asymmetry of the quantum-well confining potential and the lack of bulk inversion symmetry.

First, let us describe the situation for a planar 2DEG. At the presence of both Rashba and Dresselhaus SOI terms, the electric-field-induced spin polarization depends both on the orientation of the in-plane electric field^{21,22} and on the spin-injection direction.²³ In order to account for these dependen-

cies, we consider the general class of \mathbf{k} -linear SOI expressed by $\Omega_i(\mathbf{k}) = \alpha_{ij} k_j$, where α_{ij} are spin-orbit coupling constants.²⁴ The most studied example is a semiconductor quantum well grown along the [001] direction. Assuming that the Cartesian coordinate axes are oriented along the principal crystallographic directions, we have for the combined Rashba-Dresselhaus model $\alpha_{11} = \beta$, $\alpha_{12} = \alpha$, $\alpha_{21} = -\alpha$, and $\alpha_{22} = -\beta$, with α and β being the Rashba and Dresselhaus coupling constants, respectively. A change in the spin-injection direction is achieved by the transformation $\mathbf{\Omega}' = U\mathbf{\Omega}(U^{-1}\mathbf{k})$, with U being a rotation matrix.²³ A configuration of particular interest is obtained after a rotation around the angle $\pi/4$, which leads to the SOI couplings: $\alpha_{11} = 0$, $\alpha_{12} = \alpha - \beta$, $\alpha_{22} = 0$, and $\alpha_{21} = -(\alpha + \beta)$.

All information about electric-field effects in the spin-charge coupled electron ensemble is contained in the spin-density matrix

$$f_{s'}^s(\mathbf{k}, \mathbf{k}' | t) = \langle a_{k_s}^\dagger a_{k's'} \rangle_t, \quad (3)$$

which is calculated from quantum-kinetic equations.^{25–28} Results are derived for the physical components $f = \text{Tr} \hat{f}$ and $\hat{f} = \text{Tr}(\boldsymbol{\sigma} \hat{f})$ of the spin-density matrix²⁸ in the $\mathbf{k}, \boldsymbol{\kappa}$ representation, where $\mathbf{k} \rightarrow \mathbf{k} + \boldsymbol{\kappa}/2$ and $\mathbf{k}' \rightarrow \mathbf{k} - \boldsymbol{\kappa}/2$.

Next, let us specify our model for SOI on a cylindrical surface. The states of the second-quantized Hamiltonian for a 2DEG on a cylinder depend on the momentum k_z along the cylinder axis, the spin s , and the angle φ around the periphery.^{29–32} Accounting for the periodic boundary condition by a discrete Fourier transformation

$$a_{k_z \uparrow}(\varphi) = \sum_{m=-\infty}^{\infty} e^{im\varphi} a_{k_z m \uparrow}, \quad a_{k_z \downarrow}(\varphi) = e^{i\varphi} \sum_{m=-\infty}^{\infty} e^{im\varphi} a_{k_z m \downarrow}, \quad (4)$$

the Hamiltonian can be cast into a form given by Eq. (1) with the parabolic dispersion relation

$$\varepsilon(\mathbf{k}) = \frac{\hbar^2 \mathbf{k}^2}{2m^*} - \frac{1}{2R} \left(\alpha - \frac{\hbar^2}{4m^*R} \right) \quad (5)$$

and the vector $\mathbf{\Omega}(\mathbf{k})$ characterizing the SOI on a cylinder

$$\mathbf{\Omega}(\mathbf{k}) = \left(0, -(\alpha k_z - \beta k_\varphi), k_\varphi \left(\alpha - \frac{\hbar^2}{2m^*R} \right) - \beta k_z \right) \equiv (0, \Omega_y, \Omega_z). \quad (6)$$

The effects of an electric field on the spin polarization on a cylinder surface are most suitably studied by projecting the spin vector on a local trihedron. This transformation is achieved by

$$\mathbf{f} = \sum_{s,s'} f_{s'}^s \mathbf{S}_{ss'}, \quad (7)$$

where the matrices

$$S^\varphi = \frac{1}{2} \begin{pmatrix} 0 & ie^{2i\varphi} \\ -ie^{-2i\varphi} & 0 \end{pmatrix}, \quad S^z = \frac{1}{2} \begin{pmatrix} 1 & 0 \\ 0 & -1 \end{pmatrix},$$

$$S^r = \frac{1}{2} \begin{pmatrix} 0 & e^{2i\varphi} \\ e^{-2i\varphi} & 0 \end{pmatrix} \quad (8)$$

project to the cylinder axis (S_z), as well as to the tangential (S_φ) and normal (S_r) directions. The above-mentioned shift of wave vectors leads to the new components $k_\varphi = (m+m'+1)/2R$ and $\kappa_\varphi = (m-m')/R$.

Starting from the Hamiltonian in Eq. (1), which applies both to the planar and cylindrical 2DEGs, the spin-charge coupled kinetic equations are derived by applying the same calculational steps as in our previous work.²⁸ As there is no need to repeat this derivation, we write down the final result

$$\frac{\partial}{\partial t} f(\mathbf{k}, \boldsymbol{\kappa}|t) - \frac{i\hbar}{m^*} \mathbf{k} \cdot \boldsymbol{\kappa} f - \frac{i}{\hbar} \boldsymbol{\Omega}(\boldsymbol{\kappa}) \cdot \mathbf{f} + \frac{e}{\hbar} \mathbf{E} \cdot \nabla_{\mathbf{k}} f = \frac{1}{\tau} (\bar{f} - f), \quad (9)$$

$$\begin{aligned} \frac{\partial}{\partial t} \mathbf{f}(\mathbf{k}, \boldsymbol{\kappa}|t) - \frac{i\hbar}{m^*} (\mathbf{k} \cdot \boldsymbol{\kappa}) \mathbf{f} - \frac{2}{\hbar} \boldsymbol{\Omega}(\mathbf{k}) \times \mathbf{f} - \frac{i}{\hbar} \boldsymbol{\Omega}(\boldsymbol{\kappa}) \mathbf{f} + \frac{e}{\hbar} (\mathbf{E} \cdot \nabla_{\mathbf{k}}) \mathbf{f} \\ = \frac{1}{\tau} (\bar{\mathbf{f}} - \mathbf{f}) + \frac{\boldsymbol{\Omega}(\mathbf{k})}{\tau} \frac{\partial}{\partial \varepsilon(\mathbf{k})} \bar{f} - \frac{1}{\tau} \frac{\partial}{\partial \varepsilon(\mathbf{k})} \overline{\boldsymbol{\Omega}(\mathbf{k}) \mathbf{f}}, \end{aligned} \quad (10)$$

where the spin-orbit coupling vector $\boldsymbol{\Omega}(\boldsymbol{\kappa})$ has to be redefined for the cylinder geometry according to

$$\boldsymbol{\Omega}(\boldsymbol{\kappa}) = -(\Omega_y(\boldsymbol{\kappa}) \sin(2\varphi), \Omega_y(\boldsymbol{\kappa}) \cos(2\varphi), -\Omega_z(\boldsymbol{\kappa})). \quad (11)$$

On the right-hand side of Eq. (10) there appear spin-dependent contributions to the collision integral, which guarantee that the spin model correctly approaches the state of thermodynamic equilibrium. The quantum-kinetic equations (9) and (10) for the elements of the spin-density matrix describe a number of interesting field-dependent spin effects in a 2DEG with SOI. We mention the study of the spin-Hall effect and the related proper definition of the spin current^{28,33} as well as the identification of spin-coherent waves in the ballistic regime.^{34,35} In addition, the basic equations (9) and (10) allow the treatment of the charge-Hall effect²¹ and the anomalous Hall effect.³⁶ Related results valid for a 2DEG on a cylindrical surface are easily obtained from Eqs. (9) and (10).

Another class of field-mediated spin effects in semiconductors is covered by spin-charge coupled drift-diffusion equations that are derived from Eqs. (9) and (10) in a straightforward manner under the condition of weak SOI. Within this framework, we studied the electric-field-driven Hanle effect, spin remagnetization waves, and the influence of an electric field on the persistent spin helix.^{37,38} Here, we extend this approach by a strict identification of field-dependent spin modes from the analytical solution of spin-charge coupled drift-diffusion equations and by treating an excitation mechanism based on the optical grating technique. Specific results are obtained for the planar and the cylindrical geometries.

To establish the quasiclassical drift-diffusion picture, the coupled quantum kinetic equations are studied in the long-wavelength and low-frequency regime. Results are easily obtained for weak SOI when a physically relevant evolution period exists, in which the carrier energy is already thermalized, although both the charge and spin densities still remain inhomogeneous. We shall focus on this regime, where the following ansatz for the spin-density matrix is justified:³⁷

$$\bar{f}(\mathbf{k}, \boldsymbol{\kappa}|t) = -F(\boldsymbol{\kappa}, t) \frac{dn(\varepsilon_{\mathbf{k}})/d\varepsilon_{\mathbf{k}}}{dn/d\varepsilon_F}, \quad (12)$$

$$\bar{\mathbf{f}}(\mathbf{k}, \boldsymbol{\kappa}|t) = -\mathbf{F}(\boldsymbol{\kappa}, t) \frac{dn(\varepsilon_{\mathbf{k}})/d\varepsilon_{\mathbf{k}}}{dn/d\varepsilon_F}. \quad (13)$$

The bar over the quantities f and \mathbf{f} indicates an integration with respect to the polar angle of the vector \mathbf{k} . In Eqs. (12) and (13), $n(\varepsilon_{\mathbf{k}})$ denotes the Fermi function and $n = \int d\varepsilon \rho(\varepsilon) n(\varepsilon)$ is the carrier density with $\rho(\varepsilon)$ being the density of states of the 2DEG. By applying the outlined schema, spin-charge coupled drift-diffusion equations are straightforwardly derived for the macroscopic carrier density $F(\boldsymbol{\kappa}, t)$ and magnetization $\mathbf{M}(\boldsymbol{\kappa}, t) = \mu_B \mathbf{F}(\boldsymbol{\kappa}, t)$ (with $\mu_B = e\hbar/2m^*c$ being the Bohr magneton). We obtain the coupled set of drift-diffusion equations,

$$\left[\frac{\partial}{\partial t} - i\mu \mathbf{E} \cdot \boldsymbol{\kappa} + D\boldsymbol{\kappa}^2 \right] F + \frac{i}{\hbar\mu_B} [\boldsymbol{\Omega}(\boldsymbol{\kappa}) - \tilde{\boldsymbol{\Omega}}(\boldsymbol{\kappa})] \cdot \mathbf{M} = 0, \quad (14)$$

$$\begin{aligned} \left[\frac{\partial}{\partial t} - i\mu \mathbf{E} \cdot \boldsymbol{\kappa} + D\boldsymbol{\kappa}^2 + \hat{\Gamma} \right] \mathbf{M} - \frac{e}{m^*c} \mathbf{M} \times \mathbf{H}_{\text{eff}} - \chi (\hat{\Gamma} \mathbf{H}_{\text{eff}}) \frac{F}{n} \\ - \frac{i\mu}{2\tau c} \tilde{\boldsymbol{\Omega}}(\boldsymbol{\kappa}) F = \mathbf{G}, \end{aligned} \quad (15)$$

in which the matrix of spin-scattering times $\hat{\Gamma}$, an axial vector $\tilde{\boldsymbol{\Omega}}$, and an effective magnetic field \mathbf{H}_{eff} appear. $\chi = \mu_B^2 n'$ denotes the Pauli susceptibility and n' is an abbreviation for $dn/d\varepsilon_F$. In addition, the spin generation by an external source is accounted for by the vector \mathbf{G} on the right-hand side of Eq. (15). D and μ denote the diffusion coefficient and the mobility, which satisfy the Einstein relation $\mu = eDn'/n$.

The general structure of Eqs. (14) and (15) applies both to the planar and cylindrical geometries. The specification of the model proceeds by defining the quantities entering these equations.

Let us first specify our model of a planar 2DEG, for which we consider the general class of linear SOI expressed by $\boldsymbol{\Omega}(\mathbf{k}) = \hat{\alpha} \mathbf{k}$, with $\hat{\alpha}$ being the 2×2 matrix of spin-orbit coupling constants. For the combined Rashba-Dresselhaus model $\alpha_{11} = -\alpha_{22} = \beta$, $\alpha_{12} = -\alpha_{21} = \alpha$, we use the representation

$$\alpha = \frac{\hbar^2 K}{m} \cos(\psi + \pi/4), \quad \beta = \frac{\hbar^2 K}{m} \sin(\psi + \pi/4), \quad (16)$$

which reduces to the pure Rashba and the pure Dresselhaus SOI for $\psi=-\pi/4$ and $\psi=\pi/4$, respectively. The spin-scattering matrix has the form

$$\hat{\Gamma} = \frac{1}{\tau_s} \begin{pmatrix} 1 & \cos(2\psi) & 0 \\ \cos(2\psi) & 1 & 0 \\ 0 & 0 & 2 \end{pmatrix}, \quad (17)$$

where the spin-scattering time τ_s is given by $1/\tau_s=4DK^2$. The electric field enters the drift-diffusion equations (14) and (15) via the vector

$$\hat{\Gamma} = \frac{4Dm^*2}{\hbar^4} \begin{pmatrix} a_{11}^2 + a_{12}^2 + a_{31}^2 + a_{32}^2 & -(a_{22}a_{32} + a_{21}a_{31}) & -(a_{11}a_{21} + a_{22}a_{12}) \\ -(a_{22}a_{32} + a_{21}a_{31}) & a_{11}^2 + a_{12}^2 + a_{21}^2 + a_{22}^2 & -(a_{12}a_{32} + a_{11}a_{31}) \\ -(a_{11}a_{21} + a_{22}a_{12}) & -(a_{12}a_{32} + a_{11}a_{31}) & a_{21}^2 + a_{22}^2 + a_{31}^2 + a_{32}^2 \end{pmatrix}, \quad (20)$$

where the quantities a_{ij} are expressed by the spin-orbit coupling constants

$$a_{11} = \beta \sin(2\varphi), \quad a_{21} = \beta \cos(2\varphi),$$

$$a_{12} = -\alpha \sin(2\varphi), \quad a_{22} = -\alpha \cos(2\varphi), \quad (21)$$

$$a_{31} = -\left(\alpha - \frac{\hbar^2}{2m^*R}\right), \quad a_{32} = \beta. \quad (22)$$

The electric field is accounted for by the vector

$$\tilde{\Omega}(\boldsymbol{\kappa}) = \frac{2m^*\tau}{\hbar^2} [\Omega(\boldsymbol{\kappa}) \times \Lambda] \quad (23)$$

with

$$\Lambda = (a_{21}\mu E_\varphi + a_{22}\mu E_z, a_{31}\mu E_\varphi + a_{32}\mu E_z, a_{11}\mu E_\varphi + a_{12}\mu E_z), \quad (24)$$

and by the effective magnetic field given by

$$\mathbf{H}_{\text{eff}} = -\frac{2m^*2c}{e\hbar^2} [\Lambda + 2iD\Omega(\boldsymbol{\kappa})], \quad (25)$$

on which the strong electric-field analogy of the Hanle effect is founded.³⁹

An exact analytical solution of the spin-charge coupled drift-diffusion equation (15) for the field-induced magnetization is straightforwardly obtained for $\tilde{\Omega}(\boldsymbol{\kappa})=\mathbf{0}$. By applying a Laplace transformation with respect to the time variable t , we obtain the analytical solution

$$\mathbf{M}'_\perp = \frac{\Sigma + \hat{\Gamma}}{D_T} \left[\mathbf{Q}_\perp - \frac{e}{m^*c\sigma} \mathbf{Q}_z \mathbf{H}_{\text{eff}} \right]$$

$$- \frac{1}{\sigma D_T} \left(\frac{e}{m^*c} \right)^2 [\mathbf{H}_{\text{eff}} \times (\mathbf{H}_{\text{eff}} \times \mathbf{Q}_\perp)], \quad (26)$$

$$\tilde{\Omega}(\boldsymbol{\kappa}) = \frac{2m^*\tau}{\hbar^2} \hat{\alpha} |(\boldsymbol{\kappa} \times \mu\mathbf{E}), \quad (18)$$

and the effective magnetic field

$$\mathbf{H}_{\text{eff}} = -\frac{2m^*2c}{e\hbar^2} \hat{\alpha} (\mu\mathbf{E} + 2iD\boldsymbol{\kappa}), \quad (19)$$

which originates from the SOI.

For a 2DEG on a cylindrical surface, we treat the Rashba-Dresselhaus model, for which the symmetric matrix $\hat{\Gamma}$ of spin-scattering times has the form

$$\mathbf{M}_z = \frac{Q_z}{\sigma} + \frac{e}{m^*c\sigma} \frac{1}{D_T} \mathbf{H}_{\text{eff}} (\Sigma + \hat{\Gamma}) \mathbf{Q}_\perp$$

$$- \left(\frac{e}{m^*c\sigma} \right)^2 \frac{1}{D_T} \mathbf{H}_{\text{eff}} (\Sigma + \hat{\Gamma}) \mathbf{H}_{\text{eff}} Q_z, \quad (27)$$

where $\mathbf{M}' = \mathbf{M} - \chi \mathbf{H}_{\text{eff}}$ and $\mathbf{M}'_\perp = \mathbf{e}_z \times \mathbf{M}'$. The inhomogeneity of the transformed equation (15) for the spin-density matrix is denoted by \mathbf{Q} and has the form

$$\mathbf{Q} = \mathbf{M}(t=0) + (i\mu\mathbf{E}\boldsymbol{\kappa} - D\boldsymbol{\kappa}^2) \chi \mathbf{H}_{\text{eff}}/s + \mathbf{G}/s. \quad (28)$$

Other quantities that appear in Eqs. (26) and (27) are defined by $\Sigma = s - i\mu\mathbf{E}\boldsymbol{\kappa} + D\boldsymbol{\kappa}^2$ and $\sigma = \Sigma + g_1$ with s being the Laplace variable. The general solution in Eqs. (26) and (27) provides the basis for the study of numerous spin-related phenomena including effects of oscillating electric fields. Most important is the identification of spin excitations by treating the denominator D_T , which is given by the determinant

$$D_T = \frac{1}{\sigma} \left\{ \Sigma [\sigma^2 + (e\mathbf{H}_{\text{eff}}/m^*c)^2] + g^2 \left[\sigma + \frac{(\mu\mathbf{E})^2}{D} \right] \right\}, \quad (29)$$

where g_1 and g denote specific spin-orbit coupling constants. The cubic equation $D_T=0$ with respect to the Laplace variable $s \rightarrow -i\omega$ yields three spin-related eigenmodes that have already been studied for zero electric field $\mathbf{E}=\mathbf{0}$ and the planar geometry in Ref. 40. Field-dependent eigenstates calculated from the zeros of Eq. (29) are characterized both by the direction of the electric field and by the spin injection/diffusion direction. Most solutions of this equation describe damped resonances in the charge transport and spin polarization. However, as already mentioned, there also exist undamped excitations, which have received particular interest in recent studies. Here, we focus on these long-lived spin oscillations and study their dependence on an electric field.

III. PLANAR 2DEG

The general spin-charge coupled drift-diffusion equations, which were derived in Sec. II, are applicable both to planar and cylindrical semiconductor heterostructures with SOI. These equations cover numerous spin-related phenomena, which were partly studied previously.^{37,38} In this section, we derive additional conclusions for a planar 2DEG and focus on an optical excitation mechanism, which allows an identification of spin-related eigenmodes. The spirit of this study heavily rests on the rich physics of space-charge waves.¹³ The main part of this paper is devoted to an illustrative example of this kind of research. Results are presented in Sec. III C.

A. Amplification of an electric field by spin injection

As a first application of our general approach, the charge-current density is studied on the basis of its definition

$$\mathbf{j}(t) = -ie\nabla_{\mathbf{\kappa}}F(\mathbf{\kappa},t)|_{\mathbf{\kappa}=0}. \quad (30)$$

Taking into account Eq. (14) and the solution in Eqs. (26) and (27), the components of the conductivity tensor are straightforwardly calculated. Here, we are interested in combining the ac electric field with an external permanent spin-injection source that provides a generation rate $G_z(s)$ for the out-of-plane spin polarization.

Focusing on the linear-response regime with respect to the in-plane electric field, an analytical expression for the conductivity tensor $\hat{\sigma}$ is obtained. In accordance with the applicability of the drift-diffusion approach, the derivation is restricted to the case when the inequality $\hbar n' / \pi \ll 1$ is satisfied. For the frequency-dependent ($s \rightarrow -i\omega$) longitudinal and Hall conductivities, we obtain

$$\begin{aligned} \sigma_{yy}^{xx}(s)/\sigma_0 &= 1 \pm \frac{G_z \tau_s}{n} \\ &\times \frac{\hbar n'}{4\pi (s\tau_s + 1)(s\tau_s + 2 \cos^2 \psi)(s\tau_s + 2 \sin^2 \psi)}, \end{aligned} \quad (31)$$

$$\begin{aligned} \sigma_{yx}^{xy}(s)/\sigma_0 &= \pm \frac{G_z \tau_s \hbar n' \sin(2\psi)}{n 2\pi s\tau_s + 2} \\ &\times \left[\frac{\tau}{\tau_s} - \frac{s\tau_s + 1}{(s\tau_s + 2 \cos^2 \psi)(s\tau_s + 2 \sin^2 \psi)} \right] \end{aligned} \quad (32)$$

with $\sigma_0 = e\mu n$. Other contributions to the charge transport, which are solely due to SOI, are much weaker than the retained terms originating from spin injection. This conclusion is illustrated by the curves (a) in Fig. 1, which have been numerically calculated for the case $G_z = 0$. Weak SOI leads only to a slight deviation of the longitudinal conductivities σ_{xx} and σ_{yy} from σ_0 . The spin effect completely disappears for the special Rashba-Dresselhaus model with $\alpha = \beta$ ($\psi = 0$). The situation drastically changes, when there is an appreciable permanent spin injection, which leads to additional

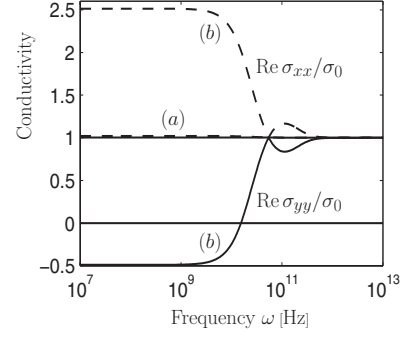


FIG. 1. Real part of the diagonal conductivity components σ_{xx} (dashed lines) and σ_{yy} (solid lines) as a function of frequency ω for $\beta/\alpha=0.5$, $\alpha=10^{-9}$ eV cm, $\tau=10^{-13}$ s, and $D=24$ cm²/s. The sets of dashed and solid lines (a) and (b) are calculated with $G_z/n=0$ and 0.03, respectively.

contributions to the steady-state charge transport owing to the spin-galvanic effect. An example is shown by the curves (b) in Fig. 1. The striking observation is that $\text{Re } \sigma_{yy}$ becomes negative for frequencies below about 10^{10} Hz. This remarkable behavior is confirmed by the expression for the static conductivity

$$\sigma_{yy}^{xx}(s)/\sigma_0 = 1 \pm \frac{G_z \tau_s \hbar n'}{n 4\pi} \cot(2\psi), \quad (33)$$

from which it is concluded that σ_{yy} changes its sign for sufficiently strong spin injection. Therefore, we meet the particular situation that a paramagnetic medium, which usually absorbs energy from an ac electric field to produce a spin accumulation, is driven to another regime, where the ac field, which propagates in a given direction, is amplified by spin injection. This stimulated emission is similar to the microwave energy gain, which was recently predicted to occur in a paramagnetic medium with sufficiently large injection spin currents.⁴¹ Based on these findings derived for rotating magnetic fields, the authors proposed a concept for a spin-injection maser. Our result is very similar to this interesting proposal.

B. Electric-field-mediated spin excitations

As a second application of our general approach, we treat coupled spin-charge eigenstates that exist in a biased sample. Effects of this kind depend not only on the directions of the electric field and the spin injection but also on the orientation of the crystallographic axes. Here, we study the influence of an electric field on an optically generated standing spin lattice that is periodic along the $\kappa_+ = (\kappa_x + \kappa_y)/\sqrt{2}$ direction. For simplicity, it is assumed that the spin generation provides a regular lattice for the out-of-plane spin polarization

$$Q_z(\kappa) = \frac{Q_{z0}}{2} [\delta(\kappa_+ - \kappa_0) + \delta(\kappa_+ + \kappa_0)]. \quad (34)$$

Inserting this source term into Eq. (27), we obtain for the related field-dependent magnetization the solution

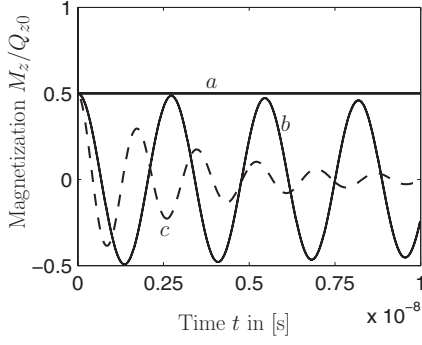


FIG. 2. Time dependence of the electric-field induced out-of-plane magnetization for $E_+ = 500$ V/cm, $D = 24$ cm²/s, and $\tau = 10^{-13}$ s. The lines a, b, and c were calculated for $\kappa_+/\sqrt{2}K = 2$ and $\alpha = \beta = 10^{-9}$ eV cm; $\kappa_+/\sqrt{2}K = 2.01$ and $\alpha = \beta = 10^{-9}$ eV cm; and $\kappa_+/\sqrt{2}K = 2.02$, $\alpha = 1.05$, and $\beta = 0.95 \cdot 10^{-9}$ eV cm, respectively. In addition, we set $r_+ = 0$.

$$M_z(\kappa, s) = \frac{\Sigma\sigma + g^2}{\Sigma[\sigma^2 + (e\mathbf{H}_{\text{eff}}/m^*c)^2] + g^2[\sigma + (\mu\mathbf{E})^2/D]} Q_z(\kappa). \quad (35)$$

The character of which is mainly determined by the poles calculated from the zeros of the denominator. The coupling constant g is given by $4Dm^{*2}|\hat{\alpha}|/\hbar^4$ and $g_1 = 2/\tau_s$. Pronounced oscillations arise for the special Rashba-Dresselhaus model with $\alpha = \beta$. In this case ($g = 0$), Eq. (35) is easily transformed to spatial and time variables with the result

$$M_z(r_+, t) = \frac{Q_{z0}}{2} \left\{ e^{-D(\kappa_0 + 2\sqrt{2}K)^2 t} \cos[\kappa_0 r_+ + \mu E_+(\kappa_0 + 2\sqrt{2}K)t] \right. \\ \left. + e^{-D(\kappa_0 - 2\sqrt{2}K)^2 t} \cos[\kappa_0 r_+ + \mu E_+(\kappa_0 - 2\sqrt{2}K)t] \right\}, \quad (36)$$

where $K = \sqrt{2}m^*\alpha/\hbar^2$ and $r_+ = (r_x + r_y)/\sqrt{2}$. In general, this solution describes damped oscillations of the magnetization. However, due to a spin-rotation symmetry, there appears an undamped soft mode when the wave-vector component κ_0 of the imprinted spin lattice matches the quantity $2\sqrt{2}K$, which is a measure of the SOI. This eigenmode leads to long-lived oscillations of the magnetization. Numerical results, calculated from Eq. (35), are shown in Fig. 2. Under the ideal condition $\alpha = \beta$ and $\kappa_0 = 2\sqrt{2}K$, the induced magnetization rapidly reaches the value $M_z = Q_{z0}/2$ (curve a) and remains constant afterward. However, any slight detuning of this special set of parameters sparks weakly damped oscillations that can last for many nanoseconds. Examples are shown by the curves b and c in Fig. 2. The importance of such spin-coherent waves, especially their potential for future spintronic applications, has recently been emphasized by Pershin.⁴² The long-lived spin waves that have been examined in this section are solely generated by an in-plane electric field. We see in them building blocks for future spintronic device applications that rely exclusively on electronic means for generating and manipulating spin.

C. Excitation of spin waves

Another wide research area that is covered by the spin-charge coupled drift-diffusion equations (14) and (15) [or their solution in Eqs. (26) and (27)] refers to the response of the spin subsystem to space-charge waves in semiconductor nanostructures. To provide an example for this kind of studies, we focus in this section on spin waves that are excited by an optically induced moving charge-density grating. Two laser beams with a slight frequency shift between them produce a moving interference pattern on the surface of the semiconductor sample that leads to a periodic generation rate for electron and holes of the form

$$g(x, t) = g_0 + g_m \cos(K_g x - \Omega t) \quad (37)$$

with a homogeneous part g_0 and a modulation g_m . K_g and Ω denote the wave vector and frequency of the grating. The generation rate $g(x, t)$ causes electron [$F(x, t)$] and hole [$P(x, t)$] density fluctuations that have the same spatial and temporal periodicity as the source $g(x, t)$. The dynamics of photogenerated electrons and holes is described by continuity equations, which encompass both carrier generation [$g(x, t)$] and recombination [$r(x, t)$] as well as drift and diffusion (see, for example, Ref. 43). If the retroaction of spin on the carrier ensemble is neglected, we obtain the set of equations

$$\frac{\partial F}{\partial t} = \frac{1}{e} \frac{\partial J_n}{\partial x} + g(x, t) - r(x, t), \quad (38)$$

$$\frac{\partial P}{\partial t} = -\frac{1}{e} \frac{\partial J_p}{\partial x} + g(x, t) - r(x, t), \quad (39)$$

where the current densities for electrons [$J_n(x, t)$] and holes [$J_p(x, t)$] are calculated from drift and diffusion contributions

$$J_n = e\mu_n E_x F + eD_n \frac{\partial F}{\partial x}, \quad (40)$$

$$J_p = e\mu_p E_x P - eD_p \frac{\partial P}{\partial x}. \quad (41)$$

In these equations, μ_n and μ_p (D_n and D_p) denote the mobilities (diffusion coefficients) for electrons and holes, respectively. A constant electric field E_0 applied along the x direction is complemented by a space-charge field $\delta E(x, t)$, which is calculated from unbalanced electron and hole densities via the Poisson equation

$$\frac{\partial E_x}{\partial x} = \frac{4\pi e}{\varepsilon} (P - F) \quad (42)$$

with ε being the dielectric constant. The optical grating leads to a weak modulation of the carrier densities around their mean value ($F = F^0 + \delta F$ and $P = P^0 + \delta P$). Due to the spin-charge coupling manifest in Eqs. (14) and (15), charge-density waves are transferred to the spin degrees of freedom and vice versa. As the hole spin relaxation is rapid, the time evolution of the generated spin pattern can be interpreted in terms of the motion of electrons alone. Consequently, the

hole density is not considered in the equations for the magnetization.

In the absence of the optical grating, there is no out-of-plane spin polarization ($F_z^0=0$). For the in-plane components, a short calculation leads to the result

$$F_x^0 = -\frac{1}{2}\hbar K_{11}\mu_n E_0 n', \quad (43)$$

$$F_y^0 = -\frac{1}{2}\hbar K_{21}\mu_n E_0 n', \quad (44)$$

which expresses the well-known effect of the electric-field mediated in-plane spin accumulation.^{44,45} In these equations, the spin-orbit coupling constants are denoted by $K_{ij} = 2m\alpha_{ij}/\hbar^2$. Besides this homogeneous spin polarization, there is a field-induced contribution, which is due to the optical grating. For the respective spin modulation, the harmonic dependence of the carrier generation in Eq. (37) via $z = K_g x - \Omega t$ remains intact. In view of the periodic boundary condition that we naturally exploit for the optically induced grating, it is expedient to perform a discrete Fourier transformation with respect to the z variable according to the prescription $F(z) = \sum_p \exp(ipz)F(p)$. The resulting equations for the Fourier coefficients of the magnetization are easily solved by perturbation theory with respect to the optically induced electric field $Y = \delta E/E_0$ and spin δF contributions. For the field-dependent homogeneous spin components ($p=0$), we obtain the solution

$$\delta F_x(0) = \frac{2K_{12}n}{g\tau_s e E_0 n'} \delta F_z(0), \quad (45)$$

$$\delta F_y(0) = \frac{2K_{22}n}{g\tau_s e E_0 n'} \delta F_z(0), \quad (46)$$

$$\delta F_z(0) = -\frac{(\mu_n E_0)^2/D_n}{2/\tau_s + (\mu_n E_0)^2/D_n} \{S(1)Y(-1) + S(-1)Y(1)\}, \quad (47)$$

in which the $p=1$ spin fluctuation occurs via the quantity

$$S(1) = \delta F_z(1) + \frac{\tau_s}{2\tau_E} \frac{K_{11}}{K_g} \delta F_y(1) - \frac{\tau_s}{2\tau_E} \frac{K_{21}}{K_g} \delta F_x(1). \quad (48)$$

The scattering time τ_E , which is provided by the constant electric field, is given by $1/\tau_E = \mu_n E_0 K_g$. The spin response described by Eqs. (45)–(48) is a consequence of electric-field fluctuations that accompany the optically induced charge modulation. As we neglect the retroaction of the induced spin fluctuation on the charge balance, the determination of $Y(p=1)$ rests exclusively on Eqs. (37)–(42). The calculation has been performed in our previous work.⁴³ To keep our presentation self-contained, we present the respective results that are needed for the calculation of the spin polarization. The relative electric-field modulation, which has the form

$$Y(1) = -\frac{g_m}{2g_0 \tau \tau_M} \frac{1 + i\Lambda_-}{(\Omega - \Omega_1)(\Omega - \Omega_2)}, \quad (49)$$

exhibits characteristic resonances at eigenmodes of space-charge waves given by

$$\begin{aligned} \Omega_{1,2} = & -\frac{1}{2}(\mu_- E_0 K_g + i\Gamma) \\ & \pm \sqrt{\left[\frac{1}{2}(\mu_- E_0 K_g + i\Gamma)\right]^2 + (1 + \alpha_1)\tau \tau_M}. \end{aligned} \quad (50)$$

The damping of this mode

$$\Gamma = D_+ K_g^2 + \frac{1}{\tau_M} + \frac{1}{\tau} \quad (51)$$

includes the Maxwellian relaxation time $\tau_M = \varepsilon/4\pi\sigma_d$ with $\sigma_d = eg_0\tau\mu_+$ and $\mu_{\pm} = \mu_n \pm \mu_p$. The parameter α_1 in Eq. (50) depends on the electric field and is calculated from

$$\alpha_1 = d_+(\Lambda_+ - \mu\Lambda_-) + \kappa d_+(1 - \mu^2 + \Lambda_+^2 - \Lambda_-^2) + \kappa\Lambda_+, \quad (52)$$

where $d_{\pm} = \mu_{\pm} E_0 K_g \tau/2$, $\Lambda_{\pm} = D_{\pm} K_g/\mu_{\pm} E_0$, $\kappa = (\varepsilon/4\pi e) \times E_0 K_g/2g_0\tau$, and $\mu = \mu_-/\mu_+$. The resonant amplification of dc and ac current components due to space-charge waves provides information useful for the determination of the lifetime and the mobilities of photogenerated electrons and holes in semiconductors.⁴³

To continue the analysis of the spin response, the set of linear equations for the $p=1$ Fourier coefficients of the spin vector must be solved. The analytical solution has the form

$$\begin{aligned} S(1) = & \frac{\hbar\tau_s n' g\tau_E}{4\tau_E^2 K_g^2 \tilde{D}_T} \left[1 + \frac{1 + 2i\Lambda}{1 + \tilde{\Sigma}\tau_s/2\tau_E} \right] (K_{11}K_{12} + K_{21}K_{22}) \\ & \times \left\{ \tilde{\Sigma}(1 + 2i\Lambda) \frac{\delta F(1)}{n} + (\tilde{\Sigma} - i)Y(1) \right\}, \end{aligned} \quad (53)$$

where $\tilde{\Sigma} = \Lambda - i(1 + \Omega\tau_E)$ and $\Lambda = D_n K_g/\mu_n E_0$. Again, the denominator \tilde{D}_T in Eq. (53) is used for the identification of electric-field-induced eigenmodes of the spin system. For the specific setup treated in this section, the general expression given in Eq. (29) reduces to the dimensionless form

$$\begin{aligned} \tilde{D}_T = & \frac{1}{\tilde{\Sigma} + 2\tau_E/\tau_s} \left\{ \tilde{\Sigma} \left[(\tilde{\Sigma} + 2\tau_E/\tau_s)^2 + \frac{K_{11}^2 + K_{21}^2}{K_g^2} (1 + 2i\Lambda)^2 \right] \right. \\ & \left. + (g\tau_E)^2 \left[\tilde{\Sigma} + \frac{2\tau_E}{\tau_s} + \frac{(1 + 2i\Lambda)^2}{\Lambda} \right] \right\}. \end{aligned} \quad (54)$$

The closed solution in Eqs. (45)–(54) for the homogeneous spin polarization, which is due to a moving optical grating, has a resonant character when eigenmodes of the spin subsystem are excited. The dispersion relations of these modes are obtained from the cubic equation $\tilde{D}_T=0$ with respect to Ω . Depending on the relative strength of the imaginary part in the equation $\Omega = \Omega(\kappa)$, a more or less pronounced resonance occurs in the induced spin polarization. Due to the spin-rotation symmetry of the model, the special Rashba-

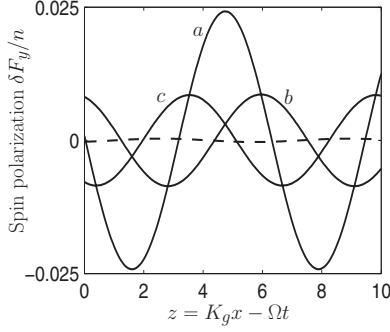


FIG. 3. Induced in-plane spin polarization as a function of $z = K_g x - \Omega t$ for $\alpha = \beta = 0.2 \times 10^{-9}$ eV cm, $g_0 = g_m = 10^{19}$ cm $^{-3}$ s $^{-1}$, $\mu_n = 0.5$ cm 2 /V s, $\mu_p = 0.2$ cm 2 /V s, $T = 77$ K, and a recombination time $\tau_r = 10^{-6}$ s. The curves a, b, and c are calculated with $E_{0 \max} = 2.67$ kV/cm, $E_{0 \max} + 100$ V/cm, and $E_{0 \max} - 100$ V/cm, respectively. For the dashed line, we used $E_0 = 1$ kV/cm.

Dresselhaus system with $\alpha = \beta$ provides an attractive example. By rotating the spin-injection direction, the situation becomes even more interesting. A rotation around $\pi/4$ leads to the set of SOI parameters $\alpha_{11} = \alpha_{12} = \alpha_{22} = 0$ and $\alpha_{21} = -2\alpha$. In this special case ($g = 0$), we obtain for the $p = 1$ Fourier component of the in-plane spin polarization the result

$$\delta F_y(1) = \frac{i\hbar n' K_{21} \Lambda [1 + (K_{21}/K_g)^2] - i(1 + \Omega \tau_E)}{2\tau_E K_g \tau_E^2 (\Omega + \Omega_{s1})(\Omega + \Omega_{s2})} Y(1), \quad (55)$$

in which two field-induced spin eigenmodes appear. The dispersion relations of which are expressed by

$$\Omega_{s1,2} = \mu_n E_0 (K_g \mp K_{21}) + iD_n (K_g \mp K_{21})^2. \quad (56)$$

Again the damping of one mode completely disappears under the condition $K_g = -K_{21} = 4m^* \alpha / \hbar^2$. This peculiarity gives rise to a pronounced resonance in the field dependence of the spin dynamics at $\mu_n E_{0 \max} = \Omega / (K_g + K_{21})$. Figure 3 illustrates this effect. Calculated is the in-plane spin modulation $\delta F_y(K_g x - \Omega t) = 2 \operatorname{Re} \delta F_y(1) \exp(iz)$. The smooth dashed line displays the response of the spin polarization to the optically generated moving charge-density pattern for $E_0 = 1$ kV/cm. The unpretentious signal is considerably enhanced under the resonance condition when $E_0 = E_{0 \max} = 2.67$ kV/cm (curve a in Fig. 3). By changing the field strength a little bit [$E_0 = E_{0 \max} + 100$ V/cm (curve b) and $E_0 = E_{0 \max} - 100$ V/cm (curve c)], the phase, amplitude, and frequency of the spin wave drastically change. This resonant influence of an electric field on the excited spin waves is a pronounced effect that is expected to show up in experiments. By applying a magnetic field, the resonant in-plane spin polarization is rotated to generate an out-of plane magnetization.

IV. CYLINDRICAL 2DEG

The general approach developed in this paper for the treatment of field-mediated spin effects in a planar 2DEG

can be transferred to the study of spin phenomena on curved surfaces. As an example, let us consider field-dependent long-lived spin modes on a cylinder. According to Eq. (29), the dispersion relation of spin waves are calculated from the equation

$$\Sigma(\sigma^2 + \omega_H^2) + g_2 \left(\sigma + \frac{(\mu E)^2}{D} \right) = 0, \quad (57)$$

in which the shorthand notations $\omega_H = (e/m^*c) \mathbf{H}_{\text{eff}}$ and $\sigma = \Sigma + g_1$ are used. The coupling constants g_1 and g_2 are given by

$$g_1 = 2 \frac{4Dm^{*2}}{\hbar^4} \left[\alpha^2 + \beta^2 - \frac{\hbar^2}{2m^*R} \left(\alpha - \frac{\hbar^2}{4m^*R} \right) \right], \quad (58)$$

$$g_2 = \left(\frac{4Dm^{*2}}{\hbar^4} \right)^2 \left[\beta^2 - \alpha \left(\alpha - \frac{\hbar^2}{2m^*R} \right) \right]^2. \quad (59)$$

The cubic equation (57) with respect to the Laplace variable s has three solutions, which give the dispersion relations of spin excitations. Most eigenmodes have a finite lifetime. However, there is one long-lived spin excitation, whose damping completely disappears for a given wave number κ_z . This mode appears for a model without any Dresselhaus SOI ($\beta = 0$) when the Rashba coupling constant α matches the quantity $\hbar^2/2m^*R$. In this case, we obtain ($s \rightarrow i\omega$)

$$\omega_{1,2} = -\mu E_z (\kappa_z \pm K) - iD (\kappa_z \pm K)^2 \quad (60)$$

with $K = 2m^* \alpha / \hbar^2$ being a wave number that is built from the Rashba spin-orbit coupling constant α . This soft mode becomes increasingly undamped in the limit $\kappa_z \rightarrow K$. The persistent spin mode of this kind, which is a consequence of a new spin-rotation symmetry, has no counterpart in the planar Rashba model and is a distinct feature that solely appears on a cylinder surface.

In order to excite the persistent spin wave, a regular lattice of spin polarization Q_r perpendicular to the cylinder surface is provided by laser pulses. For simplicity, the spin generation is assumed to have the form

$$Q_r = \frac{Q_r^0}{2} [\delta(\kappa_z - \kappa_0) + \delta(\kappa_z + \kappa_0)]. \quad (61)$$

Under the condition $Q_\varphi = Q_z = 0$, the solution of Eq. (15) is expressed by

$$M_z = \frac{\mu E_z K}{\sigma^2 + \omega_H^2} Q_r, \quad M_r = \frac{\sigma}{\sigma^2 + \omega_H^2} Q_r. \quad (62)$$

In the derivation of these equations, it was considered that the inverse Fourier transformation with respect to κ_φ leads to $\varphi = 0$. The inverse Laplace transformation and the integration over k_z give for the nonvanishing components of the field-mediated magnetization the final results

$$M_r(z, t) = \frac{Q_r^0}{2} \{ e^{-D(\kappa_0 + K)^2 t} \cos[\kappa_0 z + \mu E_z (\kappa_0 + K)t] + e^{-D(\kappa_0 - K)^2 t} \cos[\kappa_0 z + \mu E_z (\kappa_0 - K)t] \}, \quad (63)$$

$$M_z(z,t) = M_z^{(-)}(z,t) - M_z^{(+)}(z,t) \quad (64)$$

with

$$M_z^{\pm}(z,t) = \frac{\mu E_z}{(\mu E_z)^2 + (2D\kappa_0)^2} \frac{Q_{r0}}{2} \times \{2D\kappa_0 \cos[\kappa_0 z + \mu E_z(\kappa_0 \pm K)t] - \mu E_z \sin[\kappa_0 z + \mu E_z(\kappa_0 \pm K)t]\} e^{-D(\kappa_0 \pm K)^2 t}. \quad (65)$$

Both components M_z and M_r consist of a strongly and weakly damped oscillating term. Under the resonance condition $\kappa_0=K$, the first mode quickly disappears, whereas the second mode becomes completely undamped. There is a smooth dependence on the electric field E_z in the magnetization M_z along the cylinder axis. A slight detuning of the resonance, however, leads to the appearance of an electric-field-driven spin wave. The damping of which is extremely weak. The frequency of this long-lived spin excitation is directly controlled by the applied electric field. The situation is similar to the persistent spin helix of a planar 2DEG, so that the proposal of a nonballistic spin transistor⁷ supports our expectation that the robust spin wave on a cylinder and its direct manipulation by an electric field has the potential to be utilized in future spintronic device applications.

V. SUMMARY

The generation and manipulation of a spin polarization in nonmagnetic semiconductors by an electric field is a subject that has recently received considerable attention. All information needed for the description of these field-induced spin effects is given by the spin-density matrix, the equation of motion of which is governed by the model Hamiltonian. The SOI is the main ingredient in this approach. In spite of the fact that kinetic equations for the four-component spin-density matrix are straightforwardly derived, at least two caution notices are in order: (i) for the consistent treatment of scattering, its dependence on SOI must be considered and (ii) to reproduce the well-known field-induced spin accumulation, third-order spin corrections have to be retained in the kinetic equations. In order to study macroscopic spin effects, it is expedient to suppress still existing superfluous information in the spin-density matrix by deriving spin-charge coupled drift-diffusion equations. Under the condition of weak SOI, we followed this program and derived basic equations in an exact manner. These equations, which are valid for the general class of linear SOI, apply to various electric-field-induced spin effects that depend not only on the orientation of the crystallographic axes but also on the spin-injection direction and the alignment of the electric field. An exact solution of the basic equations for the magnetization

allows the identification of field-dependent spin excitations. Among these spin eigenmodes there are long-lived spin waves that can be excited by a spin and/or charge grating providing the necessary wave vector. The applicability of our general approach was illustrated by a few examples. The treatment of the spin-mediated conductivity of charge carriers reveals the possibility that a component of an ac electric field is amplified by spin injection. A similar effect led to the recent proposal for a spin-injection maser device.⁴¹ In a second application, it was demonstrated how a regular lattice of an out-of-plane spin polarization excites long-lived field-dependent spin waves in a planar 2DEG. The calculation refers to a [001] semiconductor quantum well with balanced Rashba and Dresselhaus SOIs, for which a persistent spin helix has been identified.⁶ In the main part of the paper, the rich physics of space-charge waves was utilized for the study of spin excitations. By considering a typical setup for the optical generation of a moving charge pattern, the associated dynamics of the related spin degrees of freedom was treated. It was shown that the charge modulation can be used to excite intrinsic field-dependent spin waves. This example demonstrates that the powerful methods developed in the field of space-charge waves can be used for the study of spin excitations.

Finally, we applied our approach to the treatment of spin dynamics on a curved surface, where new long-lived spin excitations exist even in the nonballistic regime. From the solution of rigorous coupled spin-charge drift-diffusion equations for a cylindrical surface, the dispersion relations of field-dependent spin eigenmodes were identified. In general, there are three damped spin excitations on a cylinder. The character of which is determined by the coupling constants α and β of the Rashba and Dresselhaus SOIs. For the pure Rashba model ($\beta=0$), a long-lived spin wave exists when the radius R of the cylinder matches the condition $R=\hbar^2/2m^*\alpha$. This finding is of particular interest as an applied electric field stimulates a nearly undamped spin wave. This peculiarity of the Rashba model on a cylindrical surface has no counterpart in a planar 2DEG. Unfortunately, the experimental demonstration of this effect is rendered more difficult because the huge internal strain within the rolled-up tube breaks the bulk inversion symmetry, so that an appreciable Dresselhaus contribution to the SOI is expected, which detunes the strong spin resonance. If this problem can be circumvented, the long-lived field-mediated spin excitations on a cylinder have the potential to be utilized in spintronic devices that work even in the nonballistic regime.

ACKNOWLEDGMENT

Partial financial support by the Deutsche Forschungsgemeinschaft is gratefully acknowledged.

*Deceased.

- ¹M. W. Wu, J. Phys. Soc. Jpn. **70**, 2195 (2001).
- ²J. L. Cheng and M. W. Wu, J. Appl. Phys. **101**, 073702 (2007).
- ³N. S. Averkiev, L. E. Golub, A. S. Gurevich, V. P. Evtikhiev, V. P. Kochereshko, A. V. Platonov, A. S. Shkolnik, and Y. P. Efimov, Phys. Rev. B **74**, 033305 (2006).
- ⁴B. Liu, H. Zhao, J. Wang, L. Liu, W. Wang, D. Chena, and H. Zhu, Appl. Phys. Lett. **90**, 112111 (2007).
- ⁵D. Stich, J. H. Jiang, T. Korn, R. Schulz, D. Schuh, W. Wegscheider, M. W. Wu, and C. Schüller, Phys. Rev. B **76**, 073309 (2007).
- ⁶B. A. Bernevig, J. Orenstein, and S. C. Zhang, Phys. Rev. Lett. **97**, 236601 (2006).
- ⁷J. Schliemann, J. C. Egues, and D. Loss, Phys. Rev. Lett. **90**, 146801 (2003).
- ⁸J. Shi, P. Zhang, D. Xiao, and Q. Niu, Phys. Rev. Lett. **96**, 076604 (2006).
- ⁹A. R. Cameron, P. Riblet, and A. Miller, Phys. Rev. Lett. **76**, 4793 (1996).
- ¹⁰S. G. Carter, Z. Chen, and S. T. Cundiff, Phys. Rev. Lett. **97**, 136602 (2006).
- ¹¹P. S. Eldridge, W. J. H. Leyland, P. G. Lagoudakis, O. Z. Karimov, M. Henini, D. Taylor, R. T. Phillips, and R. T. Harley, Phys. Rev. B **77**, 125344 (2008).
- ¹²M. Q. Weng, M. W. Wu, and H. L. Cui, J. Appl. Phys. **103**, 063714 (2008).
- ¹³M. P. Petrov and V. V. Bryksin, *Photorefractive Materials and Their Applications* (Springer, Berlin, 2007).
- ¹⁴T. Kipp, H. Welsch, C. Strelow, C. Heyn, and D. Heitmann, Phys. Rev. Lett. **96**, 077403 (2006).
- ¹⁵K.-J. Friedland, R. Hey, H. Kostial, and A. Riedel, Phys. Status Solidi C **5**, 2850 (2008).
- ¹⁶M. Trushin and J. Schliemann, Physica E **40**, 1446 (2008).
- ¹⁷O. G. Schmidt and K. Eberl, Nature (London) **410**, 168 (2001).
- ¹⁸S. Mendach, O. Schumacher, H. Welsch, C. Heyn, W. Hansena, and M. Holz, Appl. Phys. Lett. **88**, 212113 (2006).
- ¹⁹A. B. Vorob'ev, K. J. Friedland, H. Kostial, R. Hey, U. Jahn, E. Wiebicke, J. S. Yukecheva, and V. Y. Prinz, Phys. Rev. B **75**, 205309 (2007).
- ²⁰K. J. Friedland, R. Hey, H. Kostial, A. Riedel, and K. H. Ploog, Phys. Rev. B **75**, 045347 (2007).
- ²¹V. V. Bryksin and P. Kleinert, Int. J. Mod. Phys. B **20**, 4937 (2006).
- ²²M. Trushin and J. Schliemann, Phys. Rev. B **75**, 155323 (2007).
- ²³J. L. Cheng, M. W. Wu, and I. C. da Cunha Lima, Phys. Rev. B **75**, 205328 (2007).
- ²⁴O. E. Raichev, Phys. Rev. B **75**, 205340 (2007).
- ²⁵E. G. Mishchenko, A. V. Shytov, and B. I. Halperin, Phys. Rev. Lett. **93**, 226602 (2004).
- ²⁶A. A. Burkov, A. S. Nunez, and A. H. MacDonald, Phys. Rev. B **70**, 155308 (2004).
- ²⁷M. Hruska, S. Kos, S. A. Crooker, A. Saxena, and D. L. Smith, Phys. Rev. B **73**, 075306 (2006).
- ²⁸V. V. Bryksin and P. Kleinert, Phys. Rev. B **73**, 165313 (2006).
- ²⁹L. I. Magarill, D. A. Romanov, and A. V. Chaplik, Pis'ma Zh. Eksp. Teor. Fiz. **64**, 421 (1996) [JETP Lett. **64**, 460 (1996)].
- ³⁰A. V. Chaplik, D. A. Romanov, and L. I. Magarill, Superlattices Microstruct. **23**, 1231 (1998).
- ³¹L. I. Magarill, D. A. Romanov, and A. V. Chaplik, Zh. Eksp. Teor. Fiz. **113**, 1411 (1998) [JETP **86**, 771 (1998)].
- ³²M. V. Entin and L. I. Magarill, Phys. Rev. B **64**, 085330 (2001).
- ³³P. Kleinert and V. V. Bryksin, J. Phys.: Condens. Matter **19**, 476205 (2007).
- ³⁴V. V. Bryksin and P. Kleinert, Phys. Rev. B **75**, 205317 (2007).
- ³⁵P. Kleinert and V. V. Bryksin, Phys. Rev. B **76**, 073314 (2007).
- ³⁶P. Kleinert and V. V. Bryksin, Solid State Commun. **139**, 205 (2006).
- ³⁷V. V. Bryksin and P. Kleinert, Phys. Rev. B **76**, 075340 (2007).
- ³⁸P. Kleinert and V. V. Bryksin, Phys. Rev. B **76**, 205326 (2007).
- ³⁹V. K. Kalevich and V. L. Korenev, Pis'ma Zh. Eksp. Teor. Fiz. **52**, 859 (1990) [JETP Lett. **52**, 230 (1990)].
- ⁴⁰T. D. Stanescu and V. Galitski, Phys. Rev. B **75**, 125307 (2007).
- ⁴¹S. M. Watts and B. J. van Wees, Phys. Rev. Lett. **97**, 116601 (2006).
- ⁴²Y. V. Pershin, Phys. Rev. B **71**, 155317 (2005).
- ⁴³P. Kleinert, J. Appl. Phys. **97**, 073711 (2005).
- ⁴⁴V. M. Edelstein, Solid State Commun. **73**, 233 (1990).
- ⁴⁵A. G. Aronov, Y. B. Lyanda-Geller, and G. E. Pikus, Zh. Eksp. Teor. Fiz. **100**, 973 (1991) [Sov. Phys. JETP **73**, 537 (1991)].